

# Trajectory planning method of robot sorting system based on S-shaped acceleration/deceleration algorithm

Qizhi Chen<sup>1,2,3</sup>, Chengrui Zhang<sup>1,2,3</sup> , Hepeng Ni<sup>1,2,3</sup>,  
Xue Liang<sup>1,2,3</sup>, Haitao Wang<sup>1,2,3</sup> and Tianliang Hu<sup>1,2,3</sup>

## Abstract

To improve the sorting accuracy and efficiency of sorting system with large inertia robot, this article proposes a novel trajectory planning method based on S-shaped acceleration/deceleration algorithm. Firstly, a novel displacement segmentation method based on assumed maximum velocity is proposed to reduce the computational load of velocity planning. The sorting area can be divided into four parts by no more than three steps. Secondly, since the positions of workpieces are dynamically changing, a dynamic prediction method of workpiece picking position has been presented to consider all the possible positions of the robot and the workpiece, so as to realize the picking position prediction of the workpiece at any positions. Each situation in this method can constitute an equation with only one solution, and the existence of the solution can be verified by the proposed graphical method. The simulations of the motion time of the sorting process show that the proposed method can significantly shorten the sorting time and improve the sorting efficiency compared with the previous method. Finally, this method was applied to the Selective Compliance Assembly Robot Arm (SCARA) robot for experiments. In the physical picking experiment, the missing-pick rate was less than 1%, which demonstrates the efficiency and effectiveness of this method.

## Keywords

Sorting system, trajectory planning, S-shaped ACC/DEC algorithm, displacement segmentation method, dynamic prediction of workpiece picking position

Date received: 31 July 2018; accepted: 26 October 2018

Topic: Robot Manipulation and Control

Topic Editor: Andrey V Savkin

Associate Editor: Olfa Boubaker

## Introduction

The sorting for the moving workpieces, which is to identify, pick, and place the messy workpieces,<sup>1</sup> is one of the most common applications in modern industrial production.<sup>2</sup> Traditional offline programming is not applicable because the position of workpiece is random.<sup>3</sup> To achieve accurate positioning of the workpiece, machine vision is widely used in robot sorting system.<sup>4</sup> Meanwhile, the planning of sorting trajectory, which determines the smoothness, accuracy, and efficiency of sorting process, has become one of the most important factors in sorting system.<sup>5</sup>

<sup>1</sup>School of Mechanical Engineering, Shandong University, Jinan, People's Republic of China

<sup>2</sup>Key Laboratory of High Efficiency and Clean Mechanical Manufacture at Shandong University, Ministry of Education, Jinan, People's Republic of China

<sup>3</sup>National Demonstration Center for Experimental Mechanical Engineering Education, Shandong University, Jinan, People's Republic of China

### Corresponding author:

Chengrui Zhang, School of Mechanical Engineering, Shandong University, Jinan 250061, People's Republic of China.

Email: sdzucr@126.com



Creative Commons CC BY: This article is distributed under the terms of the Creative Commons Attribution 4.0 License

(<http://www.creativecommons.org/licenses/by/4.0/>) which permits any use, reproduction and distribution of the work without further permission provided the original work is attributed as specified on the SAGE and Open Access pages (<https://us.sagepub.com/en-us/nam/open-access-at-sage>).

Much work has been done about the sorting of moving workpiece. Ni et al.<sup>6</sup> planned the sorting trajectory by establishing a dynamic sorting mathematical model based on Newton–Raphson iterative method. However, the sorting speed is slow, especially for large inertia robots. Zhang et al.<sup>7</sup> proposed a method to control the conveyor speed according to the distribution density of workpieces on the conveyor to ensure that the robot is always in the fastest sorting speed. But, it is a time-consuming process to ensure high-accuracy and high-speed performances by adjusting controller parameters,<sup>8</sup> and this method is difficult to achieve and does not meet the requirements of the production cycle. Jiao et al.<sup>9</sup> realized the tracking and sorting of workpiece using the Kalman filter. But, this method sets a fixed rectangular area, and only the workpiece inside the fixed rectangular area would be sorted by the robot. This method causes a long preparation time, and the sorting efficiency is lower. Tang<sup>10</sup> applied the image technology to the dynamic target tracking and proposed to extract the workpieces coordinates by the background difference method. The image processing in this method is complicated, and the calculation time is long. The sorting efficiency cannot meet the industrial requirements. Liu et al.<sup>11</sup> realized the issue of tracking and sorting dynamic workpieces on the production line and proposed a tracking algorithm for comprehensive application of prediction targets and searching targets, enabling dynamic tracking of workpieces on conveyor. However, the method is complicated and the amount of calculation is large.

Feed rate scheduling is another key issue in robot sorting system. A lot of feed rate scheduling methods based on various acceleration/deceleration (ACC/DEC) algorithms have been proposed. The particle swarm optimization techniques have been widely used to solving motion planning problems.<sup>12,13</sup> Ni et al. proposed some feed rate scheduling methods to improve motion smoothness and efficiency based on S-shaped ACC/DEC algorithm.<sup>14,15</sup> The linear ACC/DEC algorithm<sup>16</sup> and polynomial algorithm<sup>17</sup> are also utilized to generate smooth feed rate profile. Liu et al.<sup>18</sup> used modified trapezoidal ACC/DEC method to plan the sorting trajectory of the Delta parallel manipulator. The calculation of trapezoidal ACC/DEC is simple, and the acceleration and deceleration are smooth<sup>19</sup> but the jerk is easy to overrun and it is not suitable for robot with large inertia. When the robot moves at a high speed, the inertia of the end is large, and it is easy to bring about vibration and impact, which will cause serious damage to the body and motor. S-shaped ACC/DEC algorithm with seven sections has continuous acceleration, limited jerk, and the velocity planned by S-shaped method is more stable and can effectively reduce the vibration and shock.<sup>20</sup>

To cope with these problems, this article proposes a novel trajectory planning method based on S-shaped ACC/DEC algorithm. Firstly, a novel displacement segmentation method based on assumed maximum velocity is proposed to reduce the computational load of velocity

planning. The sorting area can be divided into four parts by no more than three steps. Secondly, since the positions of workpieces are dynamically changing, a dynamic prediction method of workpiece picking position is presented to consider all the possible positions of the robot and the workpiece, so as to realize the picking position prediction of the workpiece at any positions. Each situation in this method can constitute an equation with only one solution, and the existence of the solution can be verified by proposed graphical method. Finally, the simulations and experiments of the sorting process show that the proposed method can significantly shorten the sorting time and improve the sorting efficiency compared with the previous method.

The remainder of this article is structured as follows. In the second section, the overall structure of the robot sorting system is introduced briefly. Meanwhile, the S-shaped ACC/DEC algorithm and path planning of sorting trajectory are introduced briefly. The third section develops the proposed displacement segmentation method and dynamic prediction method of workpiece picking position. The simulation and experimental results are analyzed to verify the feasibility and stability of the proposed methods in the fourth section. Finally, the article is concluded in the fifth section.

## Problem background

### Robot sorting system

As shown in Figure 1, the robot sorting system is composed of a Selective Compliance Assembly Robot Arm (SCARA) robot, two conveyor belts, a pallet, an industrial camera, and some workpieces. The sorting process can be described as follows: the scattered workpieces move on the conveyor I with a constant speed. The industrial camera collects the position information of the workpiece and transmits it to the robot controller, then the robot picks the workpiece and place them to the pallets on the conveyor II. The workpiece on the conveyor must pass through three areas completely. Firstly, the workpiece will enter the visual identification area. Secondly, the workpieces move for a while to reach the picking area, where the robot performs the grasping action. Finally, after the grasping action is completed, the robot moves directly above the pallet and then places the workpiece in the pallet, which is workpiece placement area.

### S-shaped ACC/DEC algorithm

To avoid vibration in the motion process and achieve a smoother motion curve, this article applies S-shaped ACC/DEC algorithm. The kinematic profiles of the algorithm are illustrated in Figure 2. The S-shaped curve can be divided into seven parts.<sup>21</sup> According to the specified motion parameters such as the maximum jerk  $J_{\max}$ , acceleration  $a_{\max}$ , command velocity  $F$ , motion displacement  $L$ , starting point

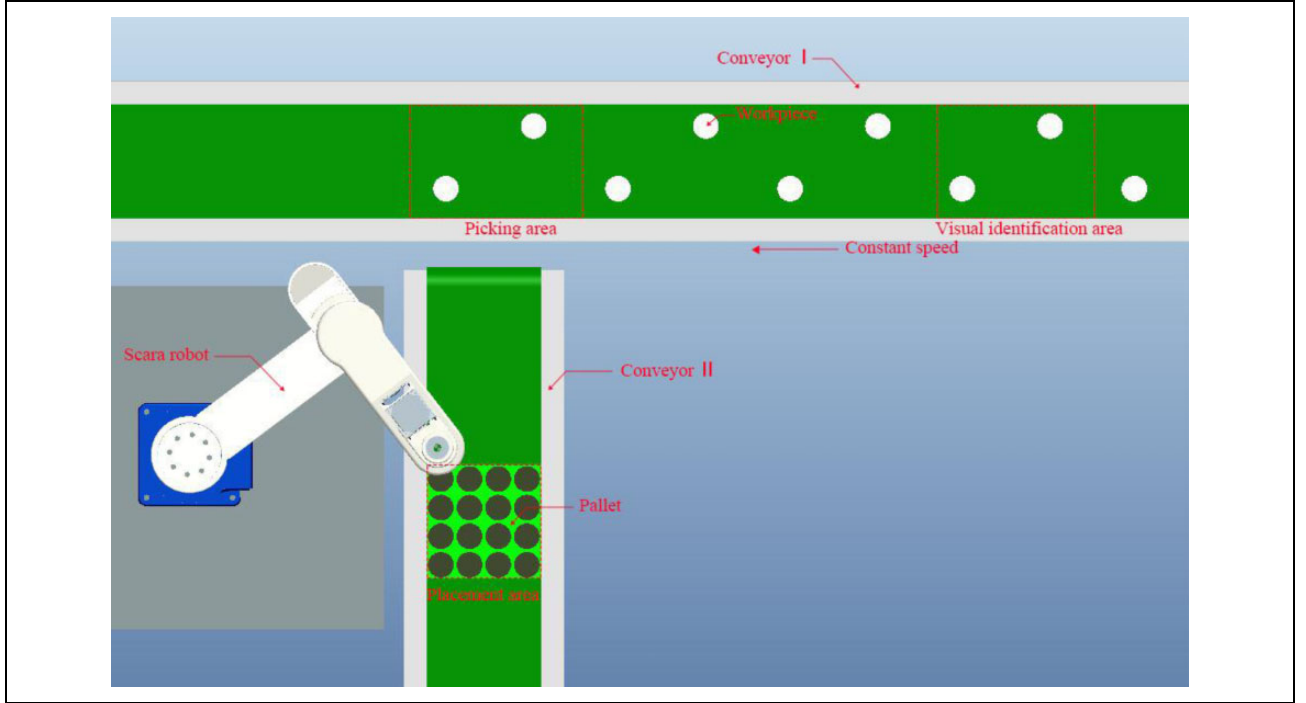


**Figure 1.** Robot sorting system model.

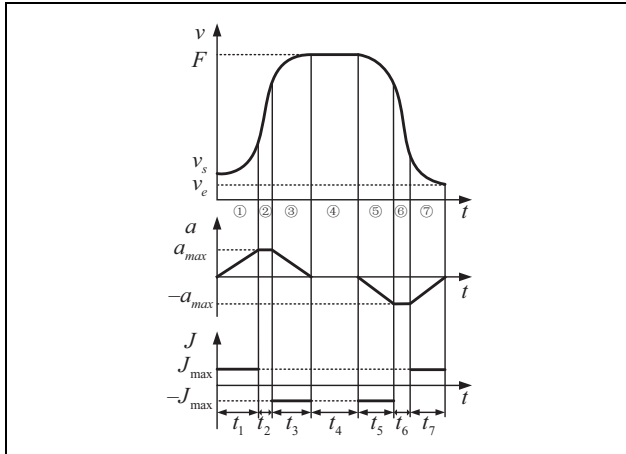


**Figure 2.** The S-shaped ACC/DEC profiles with seven sections. ACC/DCC: acceleration/deceleration.

velocity  $v_s$  and ending point velocity  $v_e$ , and the time for each section  $\{[t_1, t_2, t_3, t_4, t_5, t_6, t_7]\}$  of the feed rate profile can be calculated by analytical or numerical methods.<sup>22</sup>

### Path planning

It is a typical point-to-point (PTP) process that picks the workpiece on the conveyor I and places it in the pallet of the conveyor II.<sup>6</sup> To prevent the vibration caused by the sudden change of the trajectory at the corner, and shorten the motion time, the arc transition mode is adopted at the corner.<sup>23</sup> As shown in Figure 3, the “door” path includes three segments:  $P_1P_2(L_1)$ ,  $P_2P_3(L_2)$ , and  $P_3P_4(L_3)$ .

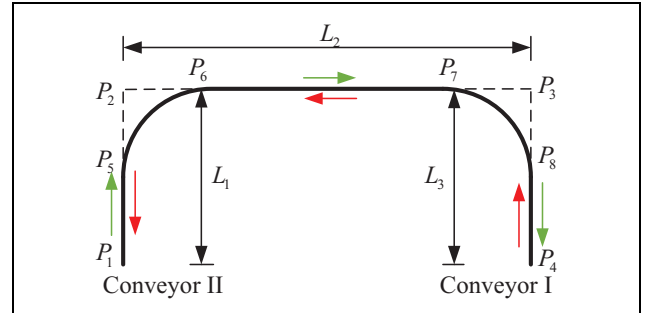


**Figure 3.** PTP path planning. PTP: point-to-point.

Let motion time of  $P_1P_2$  and  $P_3P_4$  be  $T_{up}$  and  $T_{down}$ , respectively. And the motion time of  $P_2P_3$  is  $T_{level}$ . The total motion time is

$$T_{total} = T_{up} + T_{level} + T_{down} \quad (1)$$

### Sorting trajectory planning method based on S-shaped ACC/DEC algorithm

To simplify the amount of calculation in planning trajectory of sorting, a displacement segmentation method is proposed. In addition, a dynamic prediction method of workpiece picking position is presented in detail.

#### Displacement segmentation method based on the assumed maximum velocity

In general, a typical S-shaped ACC/DEC algorithm includes seven segments. However, depending on the

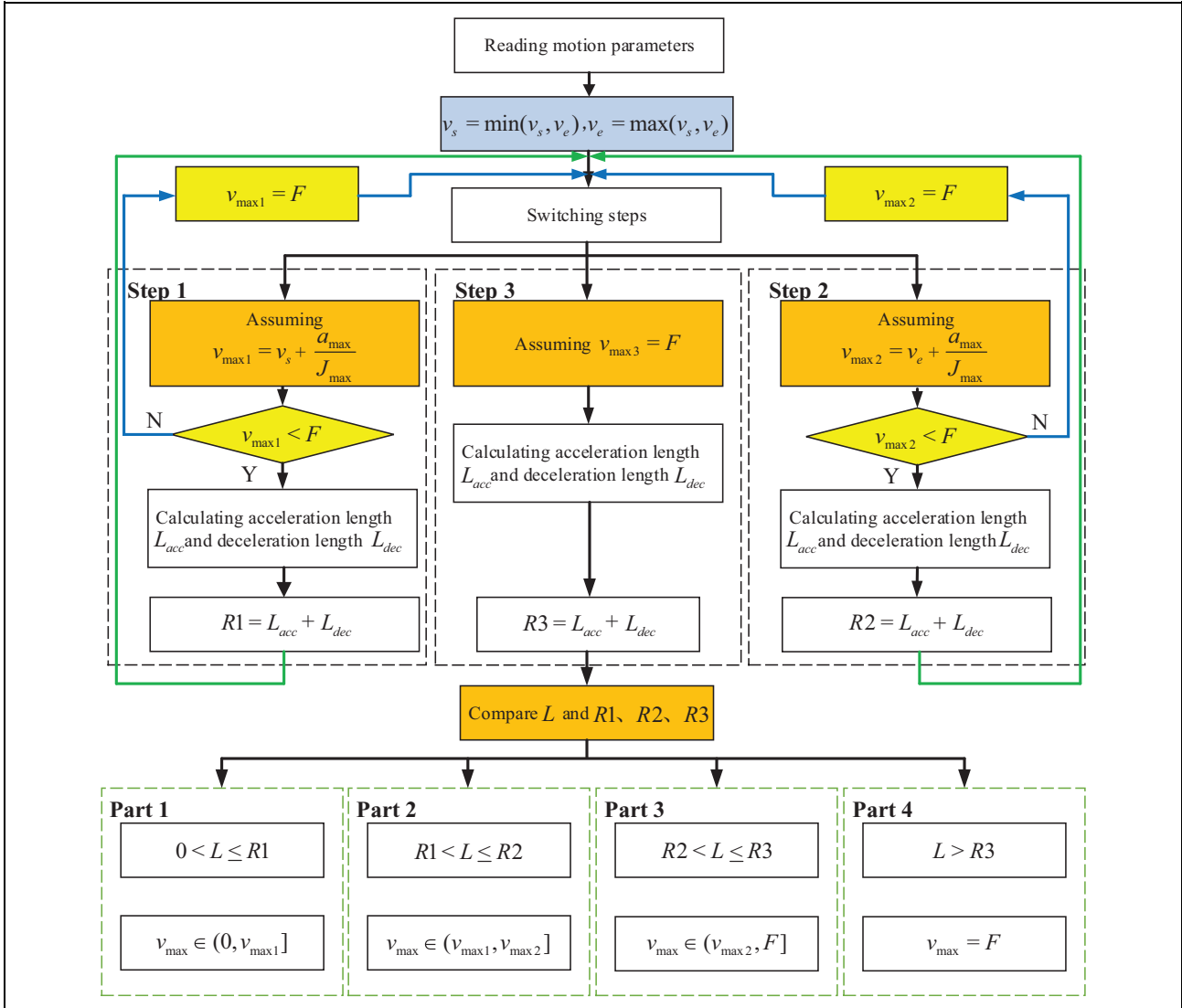


**Figure 4.** The flowchart of proposed displacement segmentation method.

giving  $v_s$ ,  $F$ ,  $v_e$ , and  $L$ , not all seven segments exist in all cases. The difference in the existence of the segments leads to difficulties in calculation. To facilitate the calculation of the sorting trajectory, this article proposes a novel displacement segmentation method based on the assumed maximum velocity. And three kinds of assumed maximum velocities are obtained based on the existence of the segments in the S-shaped algorithm.  $v_{\max}$  is set to be the actual maximum velocity. For the convenience of discussion, we set  $v_s > v_e$ . The basic principles are discussed as follows:

Firstly, if the uniform acceleration segment does not exist,  $v_{\max}$  can be calculated by

$$v_{\max} = v_s + \frac{a_{\max}}{J_{\max}} \quad (2)$$

Secondly, if the uniform deceleration segment does not exist,  $v_{\max}$  can be calculated by

$$v_{\max} = v_e + \frac{a_{\max}}{J_{\max}} \quad (3)$$

Thirdly, if the uniform velocity section exists,  $v_{\max}$  can be obtained by

$$v_{\max} = F \quad (4)$$

Thus, different existences of S-shaped segments yield three different maximum velocities. The critical point of the proposed displacement segmentation method is to calculate the corresponding displacement based on the three special maximum velocities. Firstly, three possible maximum velocities  $\{v_{\max 1}, v_{\max 2}, v_{\max 3}\}$  are assumed by equations (2) to (4). Secondly, based on the assumed maximum velocities, three corresponding displacements  $\{R1, R2, R3\}$  can be obtained by analytical or numerical methods, respectively. Thirdly, by comparing the displacement  $L$  with the magnitude of  $\{R1, R2, R3\}$ , four intervals of

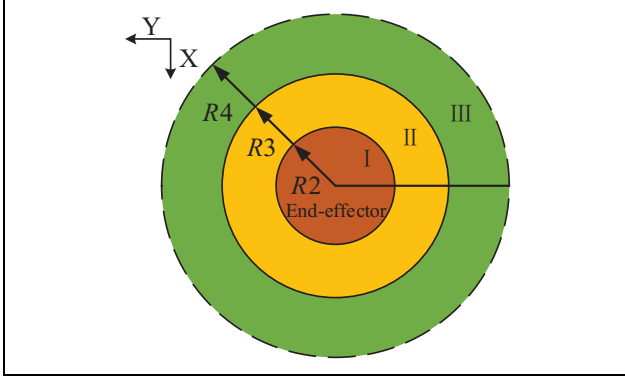


**Figure 5.** The diagram of displacement segmentation method.

displacement and corresponding maximum velocity can be achieved. As can be seen from Figure 4, the picking area is divided into four parts by no more than three steps. However,  $\{v_{\max 1}, v_{\max 2}, v_{\max 3}\}$  may be equal to each other. And in that case,  $\{R1, R2, R3\}$  may coincide. Not all four parts exist.

The “door” path is widely used as the sorting trajectory of end-effector. It requires that  $v_s$  and  $v_e$  of the sorting process are zero. So, in this situation,  $v_{\max 1} = v_{\max 2}$ ,  $R1 = R2$ , and part 2 does not exist. Then, the workspace can be divided into three parts. As shown in Figure 5. The center of the circle is the end-effector of robot and radius  $R4$  is set to be maximum workspace of robot determined by its own structure. Among the three parts:

The part I is from zero to  $R2$ , in this part,  $v_{\max} \in (0, v_{\max 1}]$ . Time of acceleration section  $t_{\text{acc}}$  and deceleration section  $t_{\text{dec}}$  can be represented by  $v_{\max}$  according to

$$\begin{cases} t_{\text{acc}} = 2\sqrt{\frac{v_{\max} - v_s}{j_{\text{lim}}}} \\ t_{\text{dec}} = 2\sqrt{\frac{v_{\max} - v_e}{j_{\text{lim}}}} \end{cases} \quad (5)$$

$L$  can be described by  $v_{\max}$  according to

$$L = \frac{v_{\max} + v_e}{2} t_{\text{acc}} + \frac{v_{\max} + v_s}{2} t_{\text{dec}} \quad (6)$$

The part II is from  $R2$  to  $R3$ , in this part,  $v_{\max} \in (v_{\max 1}, F]$ .  $t_{\text{acc}}$  and  $t_{\text{dec}}$  can be calculated according to

$$\begin{cases} t_{\text{acc}} = \frac{a_{\text{lim}}}{j_{\text{lim}}} + \frac{v_{\max} - v_s}{a_{\text{lim}}} \\ t_{\text{dec}} = \frac{a_{\text{lim}}}{j_{\text{lim}}} + \frac{v_{\max} - v_e}{a_{\text{lim}}} \end{cases} \quad (7)$$

$L$  can also be obtained by equation (6).

The part III starts from  $R3$ ,  $F$  is the actual maximum velocity in the motion process.  $t_{\text{acc}}$  and  $t_{\text{dec}}$  can be calculated according to

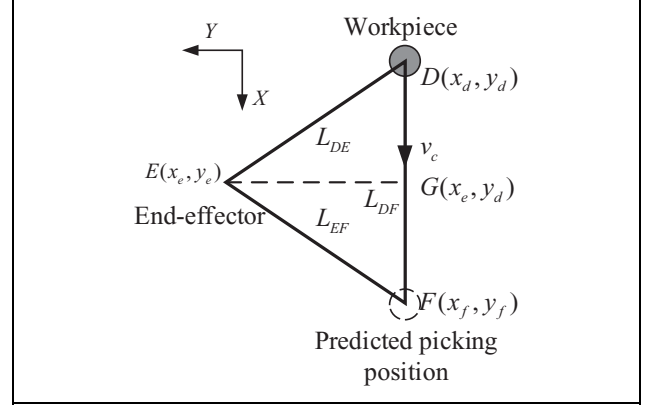


**Figure 6.** Geometric model of position prediction.

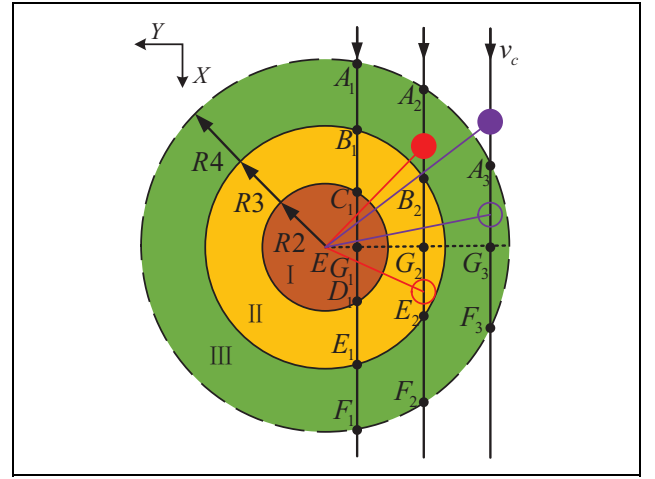


**Figure 7.** The intersection diagram of robot workspace and trajectory of workpiece.

$$\begin{cases} t_{\text{acc}} = \frac{a_{\text{lim}}}{j_{\text{lim}}} + \frac{F - v_s}{a_{\text{lim}}} \\ t_{\text{dec}} = \frac{a_{\text{lim}}}{j_{\text{lim}}} + \frac{F - v_e}{a_{\text{lim}}} \end{cases} \quad (8)$$

The time of uniform section is set to be  $t_{\text{con}} \cdot L$  in this part can be described as follows

$$L = \frac{F + v_e}{2} t_{\text{acc}} + \frac{F + v_s}{2} t_{\text{dec}} + v_{\max} t_{\text{con}} \quad (9)$$

### Dynamic prediction method of workpiece picking position

To predict the picking position of moving workpiece, the prediction method proposed by Ni et al.<sup>6</sup> is used in this article. As shown in Figure 6, it creates a geometric triangle using the coordinates of end-effector  $E(x_e, y_e)$ , the current coordinates of workpiece  $D(x_d, y_d)$ , and the predicted picking position  $F(x_f, y_f)$ . The workpiece moves on the

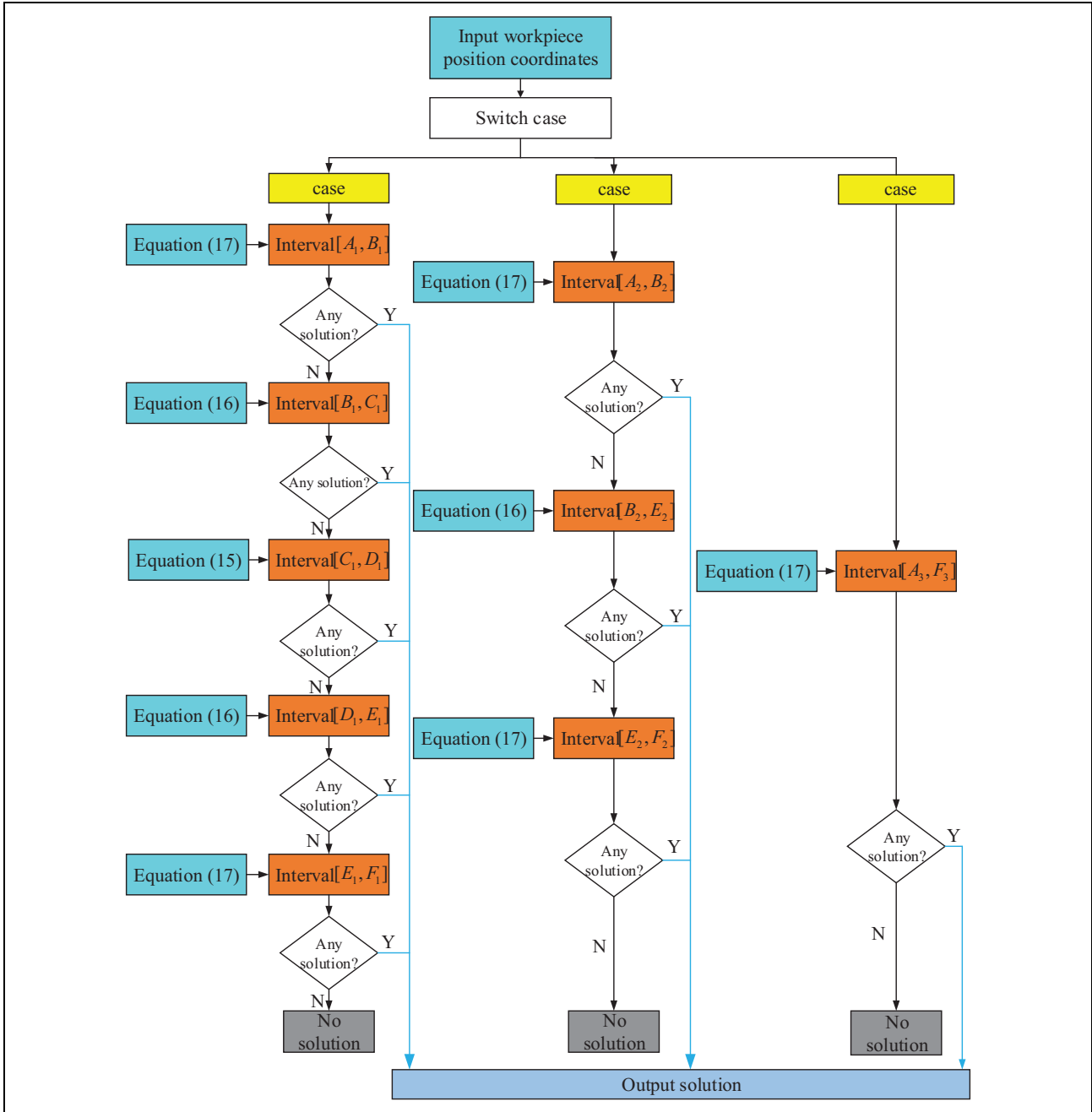


**Figure 8.** The diagram of dynamic calculation method of picking trajectory.

conveyor with a constant velocity  $v_c$  in the positive direction of  $X$ -axis.

Based on the cosine theorem of triangle, the relationship between these coordinates can be written as

$$L_{DE}^2 + L_{DF}^2 - L_{EF}^2 - 2(x_e - x_d)L_{DF} = 0 \quad (10)$$

where

$$L_{DE} = \sqrt{(x_e - x_d)^2 + (y_e - y_d)^2} \quad (11)$$

$$L_{EF} = L \quad (12)$$

$$L_{DF} = v_c T_{\text{total}} \quad (13)$$

$$T_{\text{level}} = t_{\text{acc}} + t_{\text{con}} + t_{\text{dec}} \quad (14)$$

The dynamic change of the picking trajectory mainly comes from two aspects. On the one hand, the change of the  $Y$ -axis coordinate of the workpiece determines the change of the intersection point between the motion trajectory of workpiece and the robot workspace. On the other hand, the change of the  $X$ -axis coordinate of the workpiece causes the changes of parts (I, II, or III) in Figure 5.

Therefore, the planning of the picking trajectory needs to comprehensively consider the motion trajectory of the workpiece and the end-effector. The relationship between them can be shown as Figure 7. Two possible picking situations have been described by the red and purple circles and lines. As shown in Figure 7, there may be three kinds of intersections ( $\alpha$ ,  $\beta$ ,  $\gamma$ ).

Three kinds of trajectories of workpieces intersect with robot workspace in different parts and points, and in which, points  $A_i (i = 1, 2, 3)$  are the upper boundary of the intersection area, and they are also the upper boundary of the picking area. Meanwhile, points  $F_i (i = 1, 2, 3)$  are the lower boundaries of the picking area. The analyses of the three kinds of situations are shown as follows:

In this situation,  $\alpha$ , the trajectory of workpiece intersects with the robot workspace in all the three parts (I, II, and III).  $A_1, B_1, C_1, D_1, E_1, F_1$  are critical points in this trajectory.

In this situation  $\beta$ , the trajectory of workpiece intersects with the robot workspace in part II and part III.  $A_2, B_2, E_2, F_2$  are critical points in this trajectory.

In this situation  $\gamma$ , the trajectory of workpiece intersects with the robot workspace in part III.  $A_3, F_3$  are critical points in this trajectory.

Based on the S-shaped displacement equations (5) to (9) and the prediction equations of picking position (10) to (14), the dynamic prediction equation of the workpiece picking position can be presented as follows:

#### Part I.

$$L_{DE}^2 + v_c^2(t_{acc} + t_{dec} + T_{up} + T_{down})^2 - L^2 - 2(x_e - x_d)v_c(t_{acc} + t_{dec} + T_{up} + T_{down}) = 0 \quad (15)$$

where  $t_{acc}$  and  $t_{dec}$  are obtained by equation (5),  $L$  can be calculated by equation (6).  $L_{DE}$  is easy to compute by equation (11). The calculation formula in this part contains only one unknown variable  $v_{max}$ .

#### Part II.

$$L_{DE}^2 + v_c^2(t_{acc} + t_{dec} + T_{up} + T_{down})^2 - L^2 - 2(x_e - x_d)v_c(t_{acc} + t_{dec} + T_{up} + T_{down}) = 0 \quad (16)$$

where  $t_{acc}$  and  $t_{dec}$  are obtained by equation (7),  $L$  can be also calculated by equation (6). The calculation formula in this part contains only one unknown variable  $v_{max}$ .

#### Part III.

$$L_{DE}^2 + v_c^2(t_{acc} + t_{dec} + t_{con} + T_{up} + T_{down})^2 - L^2 - 2(x_e - x_d)v_c(t_{acc} + t_{dec} + t_{con} + T_{up} + T_{down}) = 0 \quad (17)$$

where  $t_{acc}$  and  $t_{dec}$  are obtained by equation (8), and  $L$  can be obtained by equation (9). The calculation formula in this part contains only one unknown variable  $t_{con}$ . Based on the above analysis, all the calculation equations (15) to (17) only have one variable.

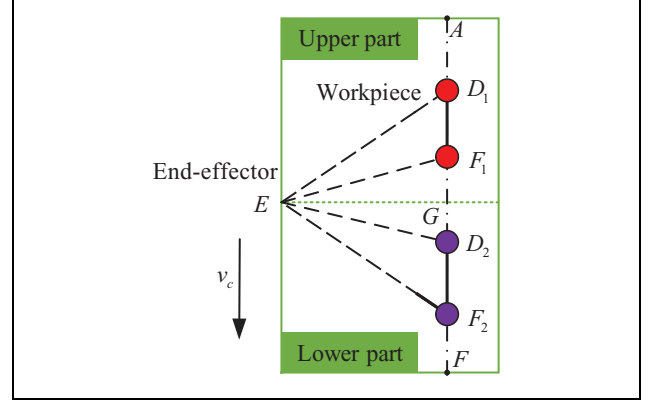


Figure 9. Simplified schematic of picking model.

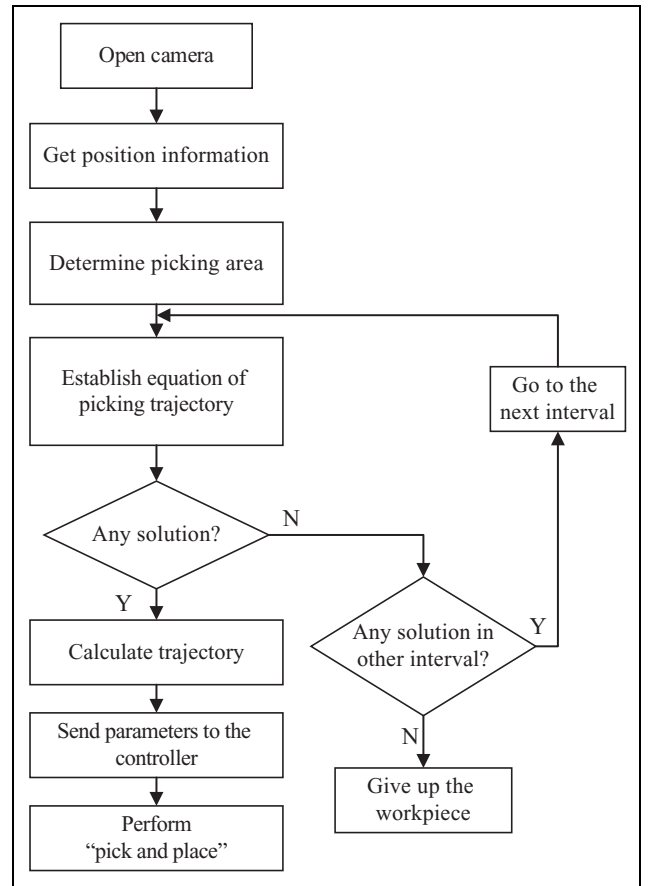
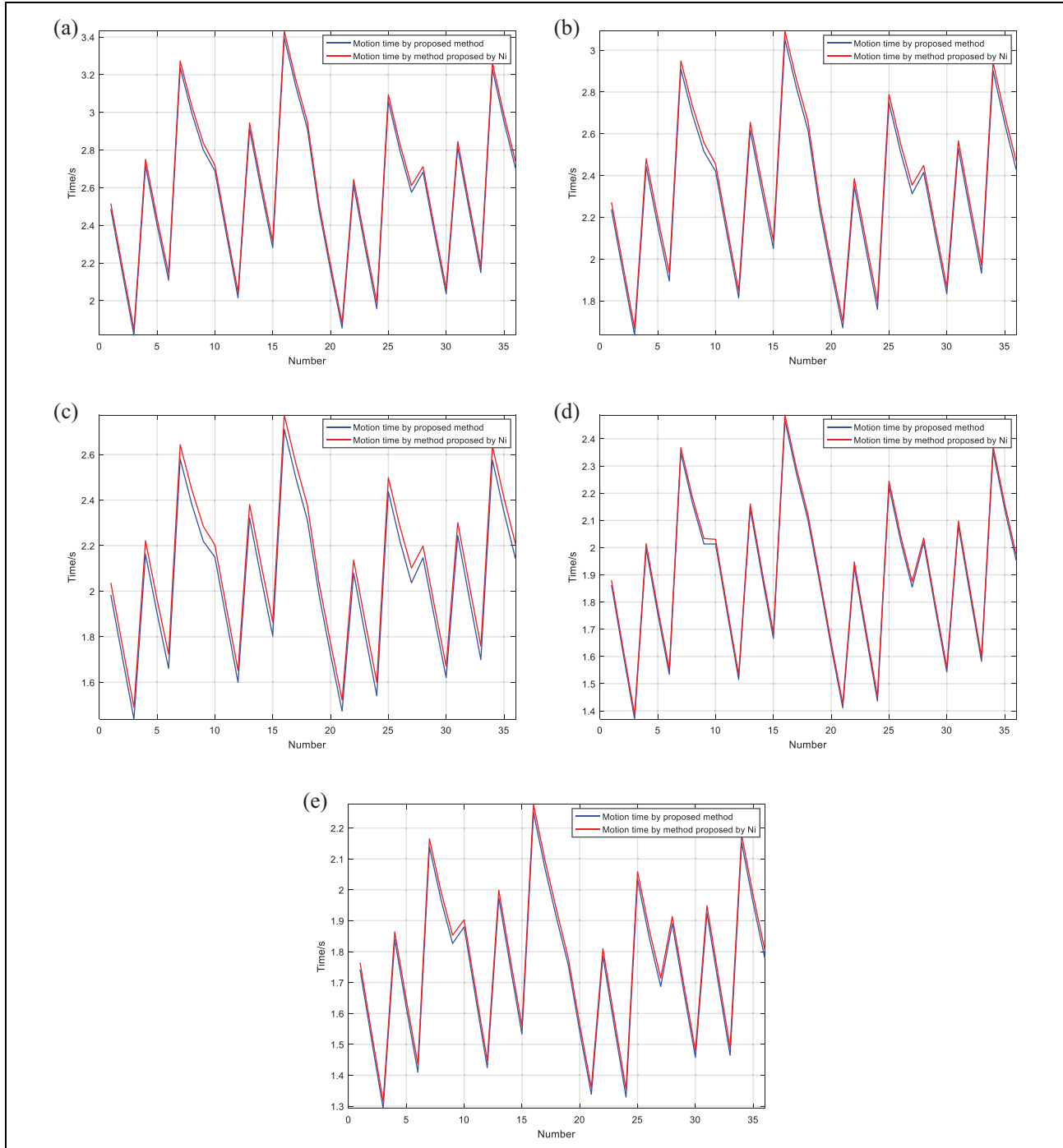


Figure 10. The operation procedure of sorting system.

Table 1. Interpolation parameters.

Serial number	$F$ (mm/s)	$a_{max}$ (mm/s <sup>2</sup> )	$J_{max}$ (mm/s <sup>3</sup> )	$v_c$ (mm/s)	$L_{up}/L_{down}$ (mm)
(a)	450	1000	15,000	100	80
(b)	500	1250	20,000	150	80
(c)	550	1500	25,000	200	60
(d)	600	1750	30,000	150	70
(e)	650	2000	35,000	100	70



**Figure 11.** The motion time of picking calculated by proposed method and method proposed by Ni et al.<sup>6</sup>

In the actual process of picking, in order to pick more workpiece in the same time, the picking time for one single workpiece should be as shorter as possible. Therefore, the picking position of the workpiece should be as close as possible to the upper limit of the picking area. As can be seen from Figure 7, intersections  $\{A_i, B_i, C_i, D_i, E_i, F_i\}$  constitute some solution intervals from the top to the bottom along the workpiece trajectory. Taking the trajectory of case  $\alpha$  as an example, there are five different intervals:

$[A_1, B_1]$ ,  $[B_1, C_1]$ ,  $[C_1, D_1]$ ,  $[D_1, E_1]$ , and  $[E_1, F_1]$ . To pick the workpiece as soon as possible, it is necessary to solve the equation (17) first in the interval  $[A_1, B_1]$ . If there is a solution in this interval, then the picking will be performed. If there is no solution in this interval, it will turn to next interval  $[B_1, C_1]$  and try to solve the equation (16). If there is no solution in the interval  $[B_1, C_1]$ , it will turn to next interval until the solution to the corresponding equation is found. The equations (15) to (17) calculated above are,



respectively, used in each interval. A clear and complete flow chart of the dynamic calculation method of picking trajectory is described as Figure 8.

It is difficult to analyze the monotonicity of equation and existence of the solution from the mathematical point of view. To avoid the complex mathematical calculation, a method based on graphic analysis was proposed to help analyze the monotonicity of equation and the existence of solutions.

A simplified schematic of picking model is shown in Figure 9, the vertical segment  $[A, F]$  is the trajectory of workpiece and workpiece moves from point  $A$  to point  $F$ . Point  $G$  is the dividing point, which divides the trajectory of workpiece into two parts: segment  $[A, G]$  is the upper part and segment  $[G, F]$  is the lower part. The position of point  $G$  changes as the position of end-effector changes, and the same is true for the position of the upper and lower part. Points  $D_1$  and  $D_2$  represent two different positions of workpieces. Point  $F_1$  indicates the picking position of  $D_1$  in the upper part, and point  $F_2$  is the picking position of  $D_2$  in the lower part. The analysis of existence of the solution is described in Appendix 1. The method proposed Appendix 1 proves the monotonicity and singularity of the equation. And this method is simple and can ensure that the only solution can be obtained by numerical method. Thus, numerical method is used to solve these equations.

## Simulation and experiment

### Simulation environment and operation procedure

When the sorting system is running, firstly, the camera captures the images of workpieces on the conveyor. Then the positions of workpieces are obtained by image processing, and its motion trajectory and the picking area are determined. After that, a dynamic prediction method of picking position is used to obtain picking trajectory in intervals shown in Figure 7. If there is a solution in the current interval, the parameters of the picking trajectory are calculated and would be sent to the robot controller. The robot performs the sorting operation. If there is no solution, it would be decided whether there are other picking intervals. The detailed procedure is shown in Figure 10.

The simulations are conducted on a personal computer with Intel(R) Core(TM) i5-4460 3.20 GHz CPU, 6.00 GB SDRAM, and Windows 7 operating system. And all the algorithms for simulations are developed and implemented on Microsoft visual studio 2013 using C++ language. The interpolation parameters (a) to (e) are listed in Table 1.

### Analysis of simulation

In the simulation, 36 sets of coordinate data including 4 coordinates of placing point and 9 coordinates of workpieces have been used. If the placing point is supposed to be fixed, the motion time of picking and placing process is

**Table 2.** Picking time and shortened time.

$F$ (mm/s)	$a_{\max}$ (mm/s <sup>2</sup> )	$J_{\max}$ (mm/s <sup>3</sup> )	Picking time by method of Ni et al. <sup>6</sup> (s)	Picking time by proposed method (s)	Shortened time (s)
400	1000	30,000	2.769	2.676	0.093
400	1100	30,000	2.688	2.612	0.076
500	1100	35,000	2.452	2.342	0.112
500	1200	35,000	2.374	2.287	0.087
600	1300	40,000	2.180	2.080	0.100
600	1400	40,000	2.116	2.036	0.080
700	1400	45,000	2.049	1.942	0.107
700	1500	50,000	1.987	1.889	0.098

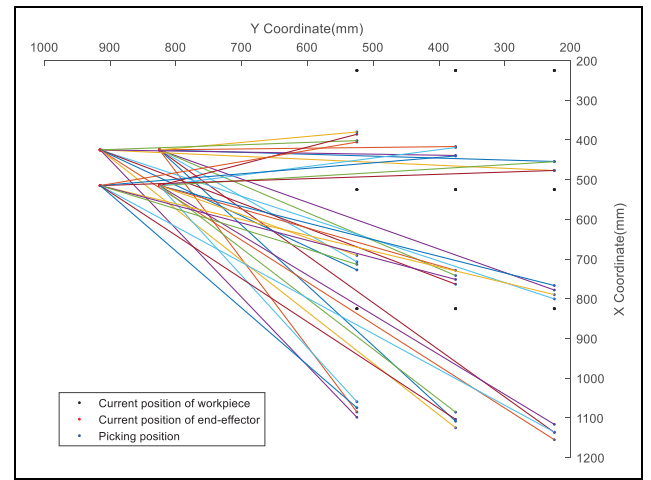


**Figure 12.** The diagram of picking trajectory obtained by proposed method.

equal. Therefore, the sorting efficiency can be expressed by calculating the picking time only. In most sorting applications, technicians generally set the conveyor speed to around 150 mm/s based on experience. Thus, the speed interval (100–200mm/s) of conveyor is chosen to test the method in practice.

To test the efficiency and robustness of the proposed method, method presented by Ni et al.<sup>6</sup> is chosen as a comparison. Ni et al.<sup>6</sup> planned the sorting trajectory by establishing a dynamic sorting mathematical model based on Newton–Raphson iterative method. The C++ programs are written by Visual studio 2013 to achieve the method presented by Ni et al.<sup>6</sup> in the same computer.

On the one hand, by substituting the same coordinate information and sampling period ( $T_s = 1$  ms), the motion time of picking process is calculated according to the parameters shown in Table 1, and the motion time profiles of two methods under five kinds of parameters are drawn respectively in Figure 11(a) to (e). Simulation results prove that the motion time calculated by proposed method is shorter than the method of Ni et al.<sup>6</sup> in the most cases.

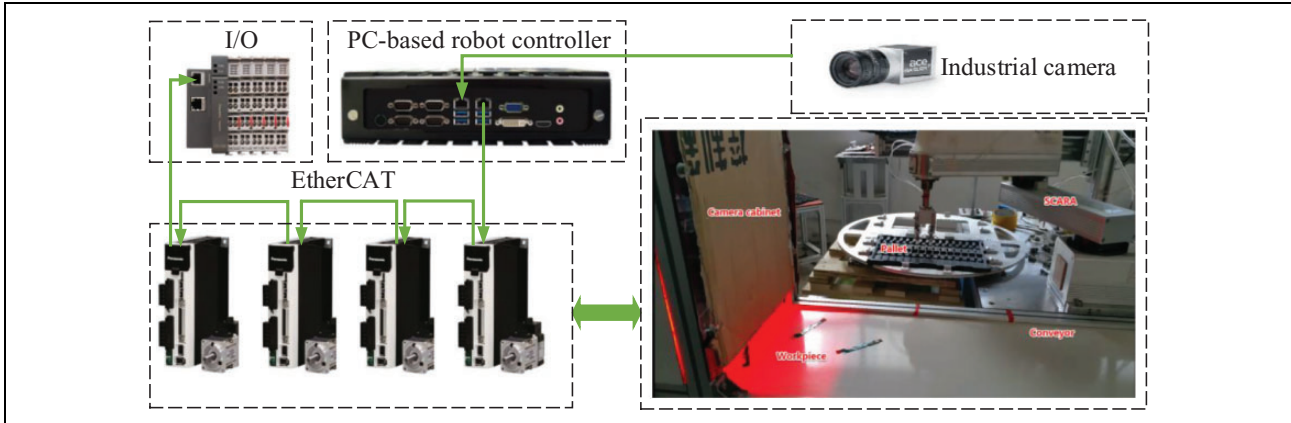


**Figure 13.** Layout of the experimental system.

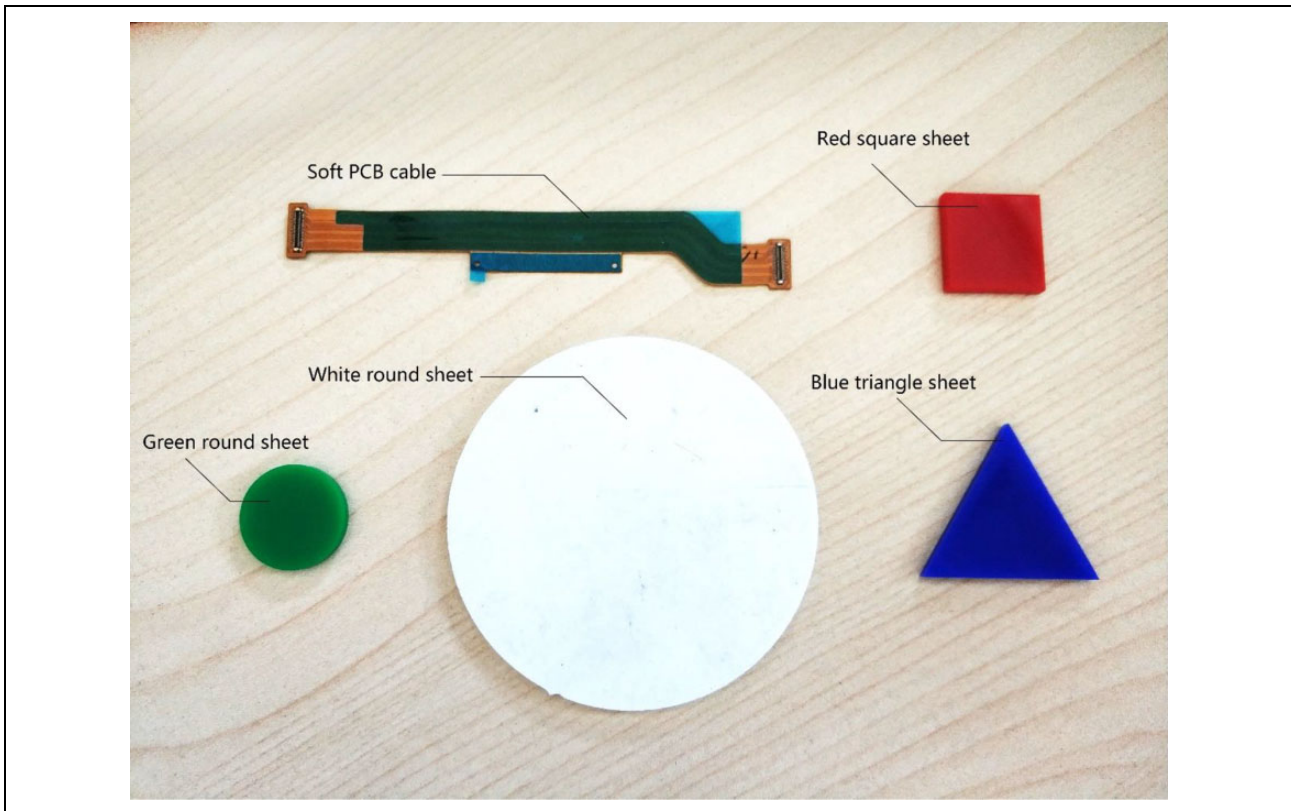


**Figure 14.** Five kinds of workpieces used in the experiment.

On the other hand, in the case where the up/down distance ( $L_{up}/L_{down} = 80$  mm) and the conveyor speed ( $v_c = 100$  mm/s) are the same, some extra motion parameters are applied to the proposed method and the method proposed by Ni et al.<sup>6</sup> to test the motion time of the picking process. As shown in Table 2, under the common motion parameters of sorting system, the picking time calculated by the proposed method is always shorter than the time calculated by the method proposed by Ni et al.<sup>6</sup> And it is the same

**Table 3.** Dimensions of workpieces.

Workpieces	Dimensions
White round sheet	Diameter: 70 mm
Green round sheet	Diameter: 20 mm
Soft PCB cable	Length: 100 mm Width: 12 mm
Red square sheet	Side length: 20 mm
Blue triangle sheet	Side length: 35 mm

PCB: printed circuit board.

**Table 4.** The result of sorting experiment.

Serial number	Total number	Workpieces	Proposed method		Method proposed by Ni <sup>6</sup>	
			Missing-pick number	Mistaken-pick number	Missing-pick number	Mistaken-pick number
(a)	500	White round sheet	0	0	0	0
(b)	500	Green round sheet	0	0	1	0
(c)	500	Soft PCB cable	1	0	2	0
(d)	500	Red square sheet	0	0	0	0
(e)	500	Blue triangle sheet	0	0	1	0

in the placing process. Thus, the high efficiency of proposed method is proven by this simulation of picking time.

To prove the stability and adaptability of the proposed method, all the picking trajectories of 36 sets of coordinate data are drawn in the Figure 12. The figure shows that a clear picking trajectory can be planned successfully for each workpiece, no matter where the robot is within the placement area.

### Experiment results

To analyze the performance of here proposed method, some picking experiments have been implemented. As shown in Figure 13, the experiment system consists of a robot system with a SCARA robot, a robot controller, a conveyor belt, and an industrial camera installed above the conveyor. The robot controller used in this article is the same as the controller used in Ni's paper.<sup>6</sup>

The model of camera is Basler acA1300-30gm, which is equipped with Sony ICX445 CCD sensor and can deliver 30 frames per second at 1.3 MP resolution. The conveyor belt is powered by a servo motor made by Panasonic. The workpiece in the experiment is the soft printed circuit board (PCB) cable inside the phone, and the end-effector of sorting robot picks up or places the workpieces by controlling the pneumatic chuck through the vacuum generator. Except for the soft PCB cable, some other shape workpieces are also tested in the experiment to verify the adaptability of the proposed method by adjusting the visual processing program according to the shape of workpiece, such as white round sheet, green round sheet, red square sheet, and blue triangle sheet. Figure 14 shows the shapes of various workpieces, and Table 3 gives the dimensions of various workpieces. To achieve a better analysis, method proposed in this article and method presented by Ni et al.<sup>6</sup> are, respectively, implemented on the experimental system with different parameters (a) to (e) shown in Table 1.

The experimental results are shown in Table 4. For both approaches, the sorting experiment is conducted five times and 500 workpieces are sorted each time. During these experiments, the number of workpieces that robots sorted amounted to 2500. For the experiment of soft PCB cable, both methods have trapped some workpieces, which may be due to the complex shape of the soft PCB cable and the accuracy problem of the visual algorithm. But for other shapes of the workpieces, the method proposed in this

article is superior to the method given by Ni et al.<sup>6</sup> in picking rate. Experimental results show that the trajectory planning method proposed in this article can ensure the sorting efficiency and accuracy of sorting system with different shaped workpieces and different interpolation parameters.

### Conclusion

The main contributions of this article include two aspects. Firstly, a novel displacement segmentation method based on assumed maximum velocity is proposed to reduce the computational load of velocity planning. The sorting area can be divided into four parts by no more than three steps. Secondly, a dynamic prediction method of workpiece picking position is presented to consider all the possible positions of the robot and the workpiece, so as to realize the picking position prediction of the workpiece at any position. Each situation in this method can constitute an equation with only one solution and the existence of the solution can be verified by proposed graphical method. The results of simulations and experiments are able to verify the high efficiency and high reliability of the proposed method. However, this study has not yet reached the end. There are still some problems that need to be studied. On the one hand, the introduction of artificial intelligence into the optimization of control parameters is an important research direction. On the other hand, it is also possible to study the method of improving the accuracy of the picking position by constructing a tracking motion strategy.


### Declaration of conflicting interests

The author(s) declared no potential conflicts of interest with respect to the research, authorship, and/or publication of this article.

### Funding

The author(s) disclosed receipt of the following financial support for the research, authorship, and/or publication of this article: The work is supported by Special Foundation for National Integrated Standardization and New Model of Intelligent Manufacturing, China (grant no. Z135060009002-132) and National Natural Science Foundation of China (grant no. 51405270).

### ORCID iD

Chengrui Zhang  <https://orcid.org/0000-0003-1536-589X>

## References

- Junyan LI, Yueqin MI, Gong J, et al. Sorting technology based on industrial robot of machine vision. *Electron Sci Technol* 2016; 29: 105–107.
- Peng G, Huang X, Wang M, et al. Moving object tracking and grasping based on visual guiding and ultrasonic measurement. *High Technol Lett* 2002; 12: 74–78.
- Wang SY, Lin H, Sun YL, et al. The research of industrial robots sorting technology based on robot vision. *Modul Mach Tool Auto Manuf Tech* 2017; 3: 125–129.
- Jiang S. *Research on industrial robot sorting system based on machine vision*. Chengdu, China: Southwest Jiaotong University, 2015.
- Li X. *Design and Research on vision sorting and tracking system of Delta parallel robot*. Guangzhou, China: South China University of Technology, 2016.
- Ni H, Liu Y, Zhang C, et al. Sorting system algorithms based on machine vision for delta robot. *Robot* 2016; 38: 49–55.
- Zhang W, Mei J, and Ding Y. Design and development of a high speed sorting system based on machine vision guiding. *Phys Proc* 2012; 25: 1955–1965.
- Mehdi H and Boubaker O. Robust impedance control-based Lyapunov–Hamiltonian approach for constrained robots. *Int J Adv Robot Syst* 2015; 2015: 190–202.
- Jiao EZ and Rong DU. Realization of sorting technology on industrial robot. *Modul Mach Tool Auto Manuf Tech* 2010; 2: 84–87.
- Tang J. *Research on robot sorting technology based on machine vision*. Nanjing, China: Nanjing Forestry University, 2011.
- Liu Z, Zhao B, Zou F, et al. Application of mean-shift and Kalman algorithms in sorting technology. *Chine J Sci Instrum* 2012; 33: 2796–2802.
- Haifa M and Olfa B. PSO-Lyapunov motion/force control of robot arms with model uncertainties. *Robotica* 2016; 34(3): 634–651.
- Mehdi H and Boubaker O. Impedance controller tuned by particle swarm optimization for robotic arms. *Int J Adv Robot Syst* 2011; 8: 93–103.
- Ni H, Hu T, Zhang C, et al. An optimized feedrate scheduling method for CNC machining with round-off error compensation. *Int J Adv Manuf Technol* 2018; 97(5–8): 1–13.
- Ni H, Yuan J, Ji S, et al. Feedrate scheduling of NURBS interpolation based on a novel jerk-continuous ACC/DEC algorithm. In: *IEEE Access*, 2018, pp. 1–1. IEEE..
- Jeon JW and Ha YY. A generalized approach for the acceleration and deceleration of industrial robots and CNC machine tools. *IEEE Trans Indus Elect* 2000; 47(1): 133–139.
- Ma Y. Study of a five-segment s-curve acceleration and deceleration algorithm. *Indus Control Comput* 2014; 2014: 60–61.
- Liu Y, Zhang C, Lang X, et al. Continuous trajectory planning for delta parallel manipulator based on matlab image recognition. *Mach Tool Hydraul* 2014; 42: 54–56.
- Wang YF, Lang XL, Zhang CR, et al. The optimal acceleration-deceleration control research of high-speed parallel manipulator. *Mach Des Manuf* 2014; 11: 85–88.
- Shi C, Zhao T, Ye P, et al. Study on S-shape curve acceleration and deceleration control on NC system. *China Mech Eng* 2007; 152: 642–663.
- Liu Z, Dong JC, Ding YY, et al. The study of S-shaped acceleration and deceleration curve and the trajectory planning strategy analysis. *Key Eng Mater* 2016; 693: 1195–1199.
- Erkorkmaz K and Altintas Y. High speed CNC system design. Part I: jerk limited trajectory generation and quintic spline interpolation. *Int J Mach Tools Manuf* 2001; 41(9): 1323–1345.
- Zhang W. *Control technique and kinematic calibration of delta robot based on computer vision*. Tianjin, China: Tianjin University, 2012.

## Appendix I

### Proof of existence of solution

**Upper part.** In this part, the workpiece moves from  $A$  to  $G$  at a constant velocity  $v_c$ . Thus, the displacement of the workpiece is monotonous and linear with the motion time.  $L_{AG}$  is the whole displacement of workpiece during the time  $T_{AG}$ , and  $T_{AG}$  is the motion time of workpiece from  $A$  to  $G$ . The curve of workpiece displacement can be shown as Figure A1. For the end-effector of robot, the displacement calculated by S-shaped acceleration/deceleration algorithm is monotonous increasing with the whole motion time. As shown in Figure A2,  $T_{EA}$  is the motion time that end-effector moves to the point  $A$ , and  $T_{EG}$  represents the time that end-effector moves to the point  $G$ .  $L_{EA}$  is the longest displacement between the end-effector and workpiece, and  $L_{EG}$  is the shortest displacement. The motion displacement of end-effector  $L_{EF_1}$  is monotonous decreasing as the point  $F_1$  changing from  $A$  to  $G$  in the upper part. Taking the displacement of the workpiece as the abscissa, the curve of the motion time of workpiece and the end-effector of robot can be represented in the  $T$ - $L$  diagram as Figure A3 based on the Figures A1 to A2.  $L_{AF_1}$  is the displacement at the intersection of two curves.

As shown in Figure A3, only if the curve of the workpiece intersects with the curve of the end effector, the equation will have a solution. Specifically, there are two situations:

If  $T_{EA} < T_{AG}$ , there is only one solution in the upper part;

If  $T_{EA} > T_{AG}$ , there may be one intersection or not. If there is no intersection in Figure A3, there may be a solution in the lower part.

### Lower part

In the lower part, the workpiece moves from  $G$  to  $F$ . Same as the upper part, the curve of displacement of workpiece can be shown as Figure A5,  $L_{GF}$  is the whole displacement of workpiece during the time  $T_{GF}$ , and  $T_{GF}$  is the motion time of workpiece from  $G$  to  $F$ . For the end-effector of robot, the displacement is monotonous increasing with the whole motion time. As shown in Figure A6,  $T_{EF}$  is the motion time that end-effector moves to the point  $F$ .  $L_{EF}$  is the longest displacement between the end-effector and

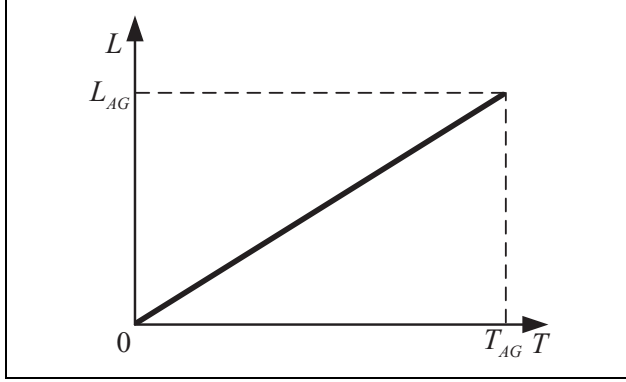


**Figure A1.** Displacement curve of workpiece.

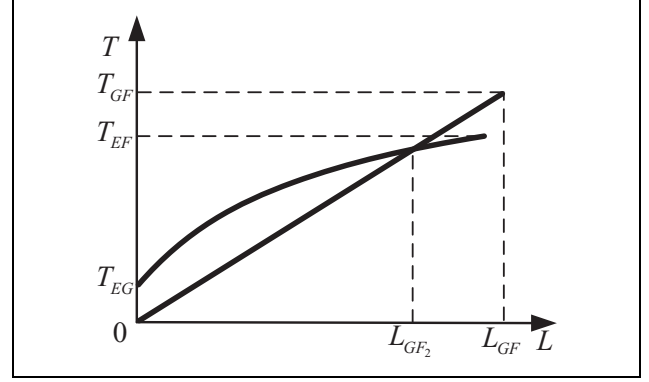


**Figure A4.** Graphical relationship in the lower part.

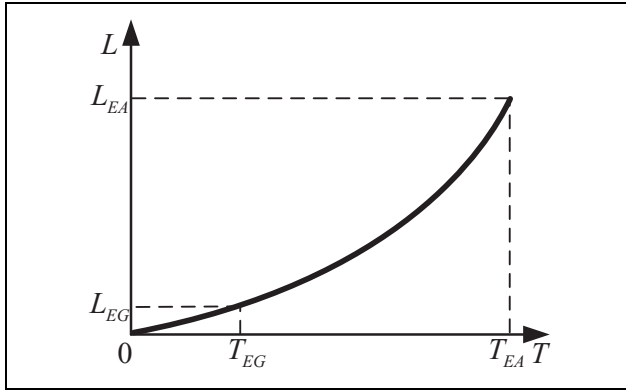


**Figure A2.** Displacement curve of end-effector.

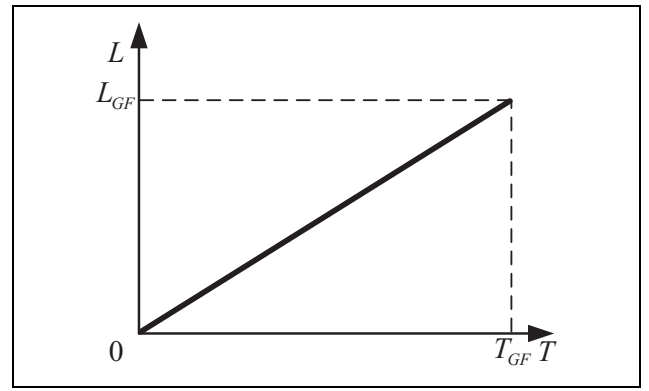


**Figure A5.** Displacement curve of workpiece.

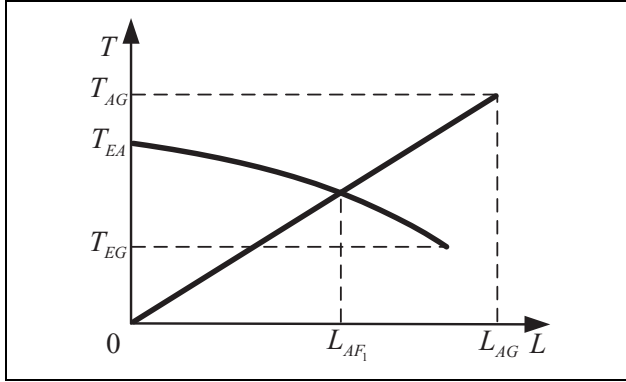


**Figure A3.** Graphical relationship in the upper part.

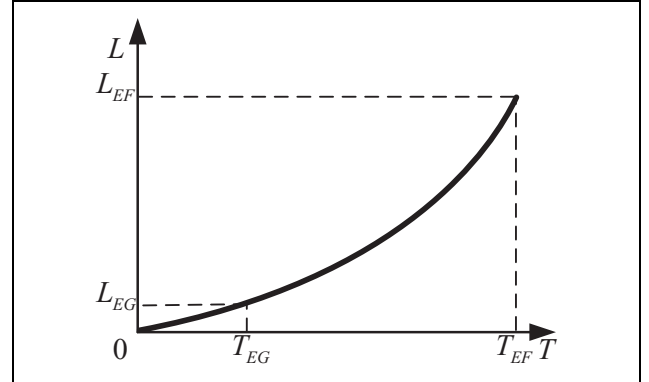


**Figure A6.** Displacement curve of end-effector.

the workpiece, and  $L_{EG}$  is the shortest displacement. However, the motion displacement of end-effector  $L_{EF_2}$  is monotonous increasing as the point  $F_2$  changing from  $G$  to  $F$ . Taking the displacement of the workpiece as the abscissa, the curve of the movement time of workpiece and the end-effector of robot can be represented in the  $T$ - $L$  diagram as Figure A4 based on the Figure A5 to Figure A6.  $L_{GF_2}$  is the displacement at the intersection of two curves.

As shown in Figure A4, only if the curve of the workpiece intersects with the curve of the end-effector, the equation will have a solution. Specifically, there are two situations:

If  $T_{EF} < T_{GF}$ , there is only one solution in the upper part;

If  $T_{EF} > T_{GF}$ , there may be one intersection or not. If there is no intersection in Figure A4, there may be no solution in the lower part.

Based on the analysis of upper part and lower part, it can be concluded that all the equations constructed by proposed prediction method only have one solution and the solution would exist in suitable situation. And this method is simple and can ensure that the only solution can be obtained by numerical method.